STATISTICS, OPTIMIZATION AND INFORMATION COMPUTING
Stat., Optim. Inf. Comput., Vol. **15**, May 2026, pp 3468–3494.
Published online in International Academic Press (www.IAPress.org)

Bayesian Estimation and Model Assessment of the Exponentiated Rayleigh Survival Model Using Laplace and MCMC Techniques: Applications with Right-Censored Medical Data

Md. Tanwir Akhtar [1,*], Najrullah Khan [2], Athar Ali Khan [3]

[1]*Department of Public Health, College of Health Sciences, Saudi Electronic University, Saudi Arabia*
[2]*Department of Community Medicine, Maharishi Markandeshwar College of Medical Sciences and Research, Ambala, Haryana, India*
[3]*Department of Statistics and Operations Research, Faculty of Science, Aligarh Muslim University, Aligarh, India*

Abstract This paper presents a comprehensive comparative study of Bayesian and classical estimation techniques for the Exponentiated Rayleigh (expRay) survival model, particularly in the presence of right-censored medical data. Using both analytic and simulation-based Bayesian methods–including Laplace approximation, Independent Metropolis (IM), and Gibbs sampling via JAGS–the model's flexibility and robustness are evaluated. Two real-world datasets, Intrauterine Device (IUD) discontinuation times and bladder cancer remission durations, are analyzed to illustrate the model's practical applications. Results from Maximum Likelihood Estimation (MLE) are benchmarked against Bayesian estimates, representing that the IM algorithm offers the best balance between computational efficiency and statistical accuracy. Model diagnostic including the posterior predictive checks (ppc) confirms the model's adequacy. The study highlights the suitability of the expRay model for modeling varying hazard rates in clinical survival data and establishes the IM-based Bayesian framework as an effective tool for medical survival analysis.

Keywords Bayesian Estimation, Exponentiated Rayleigh Distribution, Right Censoring, Laplace Approximation, MCMC Simulation, Posterior Predictive Checks, Medical Survival Data, Parametric Lifetime Models

DOI: 10.19139/soic-2310-5070-2986

1. Introduction

In the previous decades, various techniques of new generators of distribution from existing models were established and discussed. This paper adopted a novel class of distribution, called *Exponetiated Rayleigh (expRay)*, which belongs to the exponentiated family of distributions (EFDs) proposed by Gupta et al. [11]. The EFD framework introduces an additional shape parameter to an existing distribution to improve flexibility in modeling data with complex hazard structures.

Recently, a wide rage of EFDs has been proposed in the literature that include: the exponentiated transmuted Weibull distribution[5], the exponentiated-generalized-inverse-Weibull distribution (EGIWD) [10], the exponentiated-Kumaraswamy distribution and its log-transform [20], Exponentiated-T-X-family of distributions (ETXFD) with some applications [7], the Gamma-exponentiated-exponential distribution (GEED) [37], the exponentiated-Lomax distribution (ELD)[6], the exponentiated exponential distribution (EED) [26], the exponentiated-Pareto distribution (EPD) [39], the exponentiated-gamma distribution (EGD) [27], the Beta exponential distribution (BED) [29], the exponentiated-Gumbel distribution (EGD) [25], exponentiated-Frechet distribution (EFD) [28], generalized-exponential distributions [12], and the exponentiated-Weibull family (EWF) distribution [24].

*Correspondence to: Md. Tanwir Akhtar (Email: m.akhtar@seu.edu.sa). Department of Public Health, College of Health Sciences, Saudi Electronic University, Saudi Arabia.

ISSN 2310-5070 (online) ISSN 2311-004X (print)

Recent work has advanced both classical and Bayesian estimation for Rayleigh-based exponentiated models. Mahmoud & Ghazal [23] examined frequentist estimation for the expRay distribution based on generalized Type-II hybrid censored data, whereas several recent studies have advanced a Bayesian MCMC approach under the expRay distribution based on a unified hybrid censored scheme [42]. The exponentiated-Rayleigh-Poisson and exponentiated-exponential-Rayleigh families are two new exponentiated Rayleigh-type extensions and compound models that have recently emerged and demonstrated continued methodological interest and practical utility [44][45][43]. These works motivate a focused Bayesian benchmarking of the expRay model using Laplace, IM, and JAGS approaches in the present paper.

Although, these models provide useful extensions of classical distributions for modeling survival data, many lifetime models involve multiple shape or scale parameters that complicate inference, particularly under censoring and within a Bayesian framework. Contrary to this, the expRay distribution offers a simple and flexible choice by introducing only one shape parameter that allows for both increasing and decreasing hazard functions. This feature makes it well suited for survival data showing monotonic risk patterns, such as mechanical degradation or patient relapse, while maintaining a simple analytical form that facilitates Bayesian computation and MCMC implementation.

Furthermore, the expRay model retains several desirable mathematical properties: its survival and hazard functions are available in closed form, and it can be easily incorporated into regression structures through a log-link on the scale parameter. Compared with more complex members of the exponentiated family (such as the Exponentiated Weibull or Generalized Gamma), the expRay model achieves a balance between model interpretability, flexibility, and computational tractability. These characteristics make it particularly appealing for Bayesian estimation and model comparison, especially when applied to right-censored medical survival data.

Recent developments have underscored the growing importance of Bayesian survival models based on flexible lifetime distributions. For example, Bartoš et al. [48] and Paolucci et al. [49] demonstrated that Bayesian survival models using weakly informative priors can give robust and stable inference for censored biomedical data. Farhin et al. [50] further emphasized the versatility of exponentiated-type survival distributions within reliability and biomedical contexts, underscoring their capacity to represent a variety of hazard rate patterns while employing a comparatively limited number of parameters. These studies have a common line to motivate the focus of present work on the expRay model as a computationally efficient and scientifically interpretable alternative for medical survival analysis.

Accordingly, the present study develops Bayesian inference procedures for the Exponentiated Rayleigh distribution using both analytic (Laplace approximation) and simulation-based (MCMC, JAGS) techniques. The methods are validated through real-world medical datasets, for example, Intrauterine Device (IUD) data and Bladder Cancer recurrence data, and benchmarked against the classical Maximum Likelihood Estimation (MLE) approach. By doing so, this work demonstrates the flexibility of the expRay model for modeling variable hazard rates in survival data as well as its advantages in Bayesian computation relative to more complex exponentiated families.

In addition to the empirical analyses, the present work includes a comprehensive simulation study to examine the performance of estimator under multiple censoring scenarios. The study compares frequentist and Bayesian approaches using different performance metrics such as bias, RMSE, and coverage, providing a rigorous quantitative justification for the use of Bayesian paradigm in expRay survival modeling.

This study endeavors to apply Bayesian fitting to the exponentiated Rayleigh (expRay) distribution. In order to perform the Bayesian analysis of expRay distribution, weakly informative normal priors with large variance has been chosen for model parameters. Two real life time-to-event data sets – Intra-Uterine-device (IUD) data and Bladder cancer data – were considered and fitted for the purpose of illustration in order to perform Bayesian analysis of expRey model. Contrary to classical implementation, the Bayesian methods estimate the aprameter of complex survival model's parameters in a simple and effective manner. Consequently, to perform Bayesian analysis of expRay model, two critically significant techniques, asymptotic estimation and simulation methods are implemented using R packages. Asymptotic technique is applied using the R package "Laplaces Demon", which estimates the posterior results analytically, and when convergence is achieved it also provides simulated results using Sampling-Importance-Resampling (SIR) algorithm. The MCMC simulation are performed via IM algorithm

using the same package. In addition, Gibbs sampling a method of MCMC technique also performed to generate samples from the posterior density of the model paramteres through Just Another Gibbs Sampler (JAGS) using R2jags package[41].

This study develops Bayesian inference procedures for the Exponentiated Rayleigh (expRay) distribution using both analytic (Laplace approximation) and simulation-based (MCMC, JAGS) techniques. These methods are validated through real-world medical datasets and benchmarked against classical MLE, highlighting the expRay model's flexibility for modeling variable hazard rates in survival data.

2. Exponentiated Family of Distributions

Gupta et al. [11] introduced a novel family of distributions by adding a new parameter to the existing distribution. The new family has cumulative distribution function (CDF) defined as:

$$F(t) = [G(t)]^a, \quad a > 0, \tag{1}$$

and, hence, the corresponding probability density function (pdf) is given by

$$f(t) = a\,[G(t)]^{a-1}\, g(t), \tag{2}$$

where t represents the range of g and $a > 0$ is the shape parameter of the exponentiated distribution. Here, $g(t)$ and $G(t)$ denote the baseline probability density function (PDF) and cumulative distribution function (CDF), respectively.

3. Exponentiated Family of Distributions

By considering the exponentiated family of distributions as a special case of Rayleigh model. If $G(t) = 1 - \exp\{-(t/\lambda)^2\}$, then T follows $expRay(a, \lambda)$ model with shape $(a > 0)$ and scale $(\lambda > 0)$. The obtained lifetime model was proposed by Mahmoud and Ghazal [23], and exhibits quite similar characteristics to the Gamma, Weibull, and Exponentiated-Exponential distributions. In addition to the closed form nature of the CDF and PDF for this family, it offers greater flexibility in modeling hazard functions, which can increase or decrease depending on the parameter values. This flexibility—with only a single shape parameter—makes expRay computationally simpler than heavier exponentiated families (e.g., Exponentiated Weibull or Generalized Gamma) while still capturing clinically relevant monotonic hazard patterns.

The expRay(a, λ) distribution has the CDF with shape (a) and scale (λ) parameters as:

$$F(t) = \left[1 - \exp\left\{-(t/\lambda)^2\right\}\right]^a, \quad t > 0, \quad a, \lambda > 0, \tag{3}$$

And the corresponding PDF is given as:

$$f(t) = 2a\left(\frac{t}{\lambda^2}\right)\exp\left\{-(t/\lambda)^2\right\}\left[1 - \exp\left\{-(t/\lambda)^2\right\}\right]^{a-1}. \tag{4}$$

The survival function is given by:

$$S(t) = 1 - F(t) = 1 - \left[1 - \exp\left\{-(t/\lambda)^2\right\}\right]^a, \tag{5}$$

and, therefore, the hazard rate $h(t)$ can be obtained from the following relation:

$$h(t) = \frac{f(t)}{S(t)}. \tag{6}$$

Figure 1 illustrates the effect of two parameters on the probability density and survival functions of the expRay(a, λ) distribution.

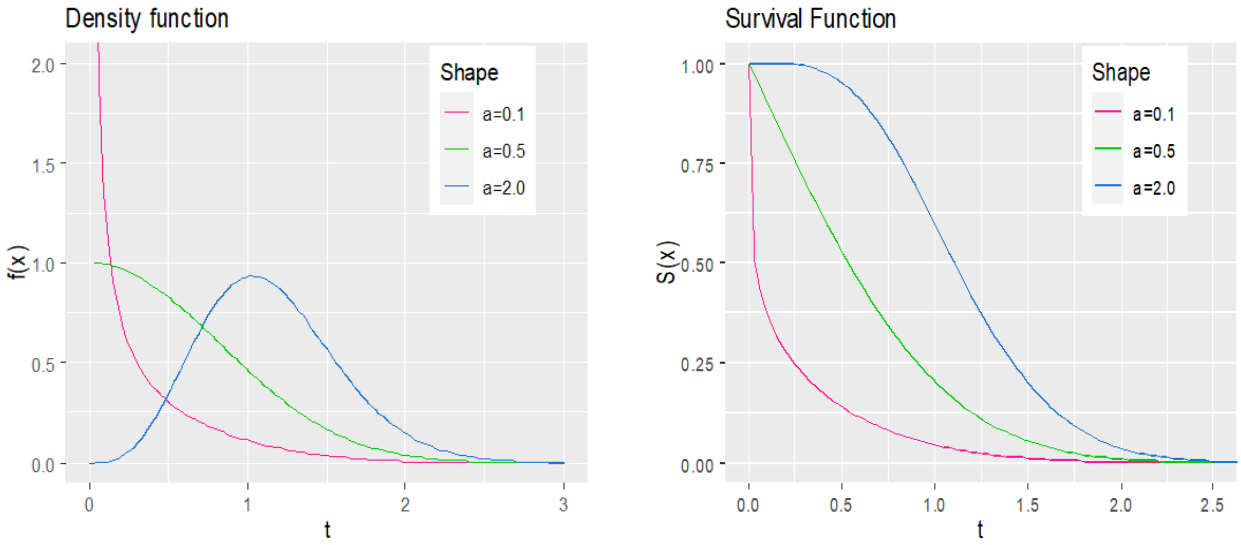

Figure 1. Left panel shows the probability density and right panel represents the survival functions of Exponentiated Rayleigh Distribution for shape parameter $a = (0.1, 0.5, 2.0)$ and scale parameter $\lambda = 1$.

3.1. Likelihood function of expRay model with censoring

The likelihood function must accommodate both observed and censored events when dealing with right-censored survival data. For a dataset of size n, where each observation is accompanied by a censoring indicator variable δ_i, the likelihood function is given by:

$$L = \prod_{i=1}^{n} [f(t_i)]^{\delta_i} [S(t_i)]^{1-\delta_i}, \tag{7}$$

Here, $\delta_i = 1$, if the event is observed (uncensored) and $\delta_i = 0$ if the observation is right-censored.

By substituting the expRay(a, λ) expressions for the PDF and survival function, the likelihood becomes:

$$L = \prod_{i=1}^{n} \left\{ 2a \left(\frac{t_i}{\lambda^2} \right) \exp\left\{-(t_i/\lambda)^2\right\} \left[1 - \exp\left\{-(t_i/\lambda)^2\right\}\right]^{a-1} \right\}^{\delta_i} \left\{1 - \left[1 - \exp\left\{-(t_i/\lambda)^2\right\}\right]^{a}\right\}^{1-\delta_i}. \tag{8}$$

The above expression serves as the basis for both maximum likelihood estimation (MLE) and Bayesian estimation of the model parameters and under censoring.

4. Estimation Methods Used

4.1. Maximum Likelihood Estimation Method

First, we considered classical maximum likelihood estimation (MLE) method to estimate our model's parameters. By optimizing the model's likelihood function defined in equation (8), one can estimate unknown parameters of a statistical model using the MLE technique. Suppose $t = (t_1, t_2, \ldots, t_n)$ represents a set random values of size n from $expRay(a, \lambda)$ distribution, then the logarithm of likelihood function, say $l(.)$, for the paramter vector

$\Theta = (a,\ \lambda)$ can be written as:

$$l(\Theta \mid \mathbf{t}) = \sum_{i=1}^{n} \left(\delta_i \Big[\log(2) + \log(a) + \log(t_i) - 2\log(\lambda) - \left(\frac{t_i}{\lambda}\right)^2 - (a-1)\log\left\{1 - \exp\left[-\left(\frac{t_i}{\lambda}\right)^2\right]\right\} - \log\left[1 - \left\{1 - \exp\left[-\left(\frac{t_i}{\lambda}\right)^2\right]\right\}^a\right]\Big] + \log\left[1 - \left\{\exp\left[-\left(\frac{t_i}{\lambda}\right)^2\right]\right\}^a\right] \right) \tag{9}$$

Next, differentiating the equation (9) w.r.t. parameters a and λ, respectively, and then equating them to zero gives

$$\frac{\partial l}{\partial a} = \sum_{i=1}^{n} \left(\delta_i \left[\frac{1}{a} - \log\{1 - \exp[-(t_i/\lambda)^2]\} \right] + (1-\delta_i) \left[\frac{(t_i/\lambda)^2 \{\exp[-(t_i/\lambda)^2]\}^a}{1 - \{\exp[-(t_i/\lambda)^2]\}^a} \right] \right) = 0, \tag{10}$$

$$\frac{\partial l}{\partial \lambda} = \sum_{i=1}^{n} \left(\delta_i \left[\frac{2t_i^2}{\lambda^3} - \frac{2}{\lambda} + \frac{2(a-1)t_i^2 \exp[-(t_i/\lambda)^2]}{\lambda^3\{1 - \exp[-(t_i/\lambda)^2]\}} \right] + (1-\delta_i) \left[\frac{2at_i^2 \{\exp[-(t_i/\lambda)^2]\}^a}{\lambda^3[1 - \{\exp[-(t_i/\lambda)^2]\}^a]} \right] \right) = 0, \tag{11}$$

By calculating the likelihood equations (10) and (11), one can obtain the MLEs of $\Theta = (a, \lambda)$, say $\hat{\Theta} = (\hat{a}, \hat{\lambda})$. Since, these equations are not in closed form and therefore much complicated to obtain an analytical expression of these estimates to compute numerically. This difficult task can be completed by using a convenient nonlinear optimization algorithm, such as Nelder–Mead, quasi–Newton, or Box–constrained optimization via the L–BFGS–B algorithm. The large sample approximation is applied to generate the statistics SE (Standard Errors) and asymptotic CI (confidence intervals). The distribution of $\hat{\Theta}$ is estimated by the bivariate–normal distribution $N\Big(0, I^{-1}(\hat{\Theta})\Big)$ with observed information matrix $I(\hat{\Theta})$ acquired at $\hat{\Theta}$. Practically, we applied `optimx()` function of R [31] to estimate the observed information matrix by using its `hessian` option. The results show this method works well and applied it for both our real data sets.

4.2. Bayesian Estimation Methods

This section discusses the Bayesian estimations of a and λ and credible interval constructions. In recent years, the Bayesian technique has attracted considerable attention for analyzing time-to-event data [30]. This approach utilizes prior knowledge about parameters and updates this information with the observed data through the posterior distribution.

The Bayes estimators are derived under the assumption that the random variables a and λ (through its regression parameterization) are independent and assigned weakly informative priors (WIPs). WIPs provide a conservative representation of prior uncertainty and allow the data to dominate the posterior. In this work, we adopted the half-Cauchy with a large scale value $HC(25)$ and unifrom $U(0, 100)$ distributions as WIPs for a parameter, whereas the normal distribution with sufficiently large variance $N(0, 1000)$ for β regression parameters. Mathematically, the half-Cauchy with scale 25 can be expressed as [1][2][16]:

$$p(a) = \frac{2 \times 25}{\pi(a^2 + 25^2)}.$$

In our model, since λ is positive, log of link function is used to cover the whole real line, that is,

$$\log(\lambda_i) = X_i^T \beta;$$

where, X denotes the model matrix and β shows the vector of regression coefficients with weakly informative Normal priors

$$\beta_j \sim N(0, 1000), \qquad j = 1, \ldots, J.$$

To ensure that the posterior inferences remain unaffected by the selection of WIPs, a prior sensitivity analysis were performed, assessing Half-Cauchy(25), Uniform$(0, 100)$, and Gamma$(0.1, 0.1)$ priors for parameter 'a'. Posterior

estimates exhibited stability for all alternatives ($< 3\%$ variation), thereby affirming the robustness of our selected priors.

Now applying the Bayes' theorem, the joint density of posterior can be expressed as

$$\begin{aligned} p(\beta, a \mid t, X) &\propto L(t, X \mid \beta, a) \times p(\beta) \times p(a) \\ &\propto \prod_{i=1}^{n} \left[2a(t/\lambda)^2 \exp\{-(t/\lambda)^2\} \left[1 - \exp\{-(t/\lambda)^2\}\right]^{a-1} \right]^{\delta_i} \\ &\quad \times \left[1 - \left[1 - \exp\{-(t/\lambda)^2\}\right]^{a}\right]^{1-\delta_i} \times \prod_{j=1}^{J} \left[\frac{1}{\sqrt{2\pi \times 10^3}} \exp\left(-\frac{1}{2} \frac{\beta_j^2}{10^3} \right) \right] \times \frac{2 \times 25}{\pi(a^2 + 25^2)}. \end{aligned} \tag{12}$$

In general, it is not feasible to obtain a closed-form expression for the ratio of the integrals presented in equation (12). In such cases, we depend on Markov Chain Monte Carlo (MCMC) techniques to draw samples from the posterior distributions. These simulated samples are then utilized to determine the Bayes estimates of model's unknown parameters and associated credible intervals. This approach helps us to deal with such a complex numerical integrations, particularly in the presence of censoring mechanisms, using tools such as the `LaplaceApproximation`, `LaplacesDemon`, and `jags` functions in R.

5. Approximation Methods Used

5.1. The Laplace Approximation

Statistical computation specialy in Bayesian analysis usually involves the calculation of complex and high-dimensional integrals. A well known Laplace Method that is a family of asymptotic approaches used to approximate such complex integrals. The marginal posterior distributions and unimodal posterior moments can be accurately estimated using Laplace's method in numerous scenarios. In particular, the posterior mode–which is expected to be unimodal and Gaussian–is calculated for every parameter. In a Gaussian distribution, the posterior mean and posterior mode are equal, and the variance is estimated [3][4][40].

Evaluation of finite integrals of the kind

$$I_n = \int_{\mathbb{R}^m} e^{-g_n(x)}\, dx, \tag{13}$$

often involve in advanced statistical application. Here, for an m-dimensional real vector $x \in \mathbb{R}^m$, $g(x)$ is a smooth and concave real function that is indexed by $n > 0$. In Bayesian analysis, for instance, $-g(\cdot)$ might represent the log-likelihood or the log-posterior kernel, and the integral I_n corresponds to Bayesian marginal likelihood or the posterior normalizing constant.

Although integral of the form (13) is often unsolvable and there are several ways to approximate it, one of which is the Laplace approximation. Assuming $\hat{x} = (\hat{x}_1, \hat{x}_2, \ldots, \hat{x}_m)$ is the unique minimum of $g(\cdot)$, where n is omited from I_n, $g_n(\cdot)$, and associated terms to simplify notation. Furthermore, we suppose that the Hessian matrix of $g(\cdot)$ at $\hat{x}$, that is,

$$\hat{A} = A(\hat{x}) = \left. \frac{\partial^2 g(x)}{\partial x\, \partial x'} \right|_{x=\hat{x}}$$

is positive definite. Thus, the Laplace approximation of integral given in equation (10) is 2nd order accurate, $I = \hat{I}[1 + O(1/n)]$ with

$$\hat{I} = \sqrt{(2\pi)^m}\, |\hat{A}|^{-1/2} e^{-g(\hat{x})}$$

as established by Bleistein and Handelsman [8] and further refined by Ruli et al. [38]. This approximation is highly effective for evaluating marginal likelihoods in Bayesian analysis when the posterior is well-behaved.

5.2. Markov chain Monte Carlo: Independent Metropilis Algorithm

In recent years, Markov Chain Monte Carlo (MCMC) methods have become widely used, particularly within the context of Bayesian estimation, to evaluate high-dimensional and analytically intractable integrals. A typical challenge involves generating samples from a target distribution, say $p(y)$. Despite the functional form of $p(\cdot)$ is known, directly sampling from it may be complicated or infeasible due to its complexity or the high dimensionality nature of y. MCMC addresses this issue by constructing a Markov chain whose invariant (stationary) distribution is $p(\cdot)$, thus enabling effective approximation through iterative sampling [21].

There are two essential processes for MCMC algorithms: the first one uses a series of generation from distinct subsets of x to simplify high dimensional issues, and the second approach uses an accept or reject rule to "correct" an arbitrary Markov chain in order to ensure the invariant distribution of $p(y)$. The first approch align with the concept behind the Gibbs sampler, whereas the second corresponds to the well-known Metropolis–Hastings (MH) algorithms. In this algorithm a proposal (or candidate) distribution is selected based on the current state of the random variables, y^k. The algorithm proceeds in two main steps: first, a proposed value, y^*, drawn from the distribution, $q(y^* \mid y^k)$; second, the proposed value is then accepted as the next state with the probability

$$\alpha(y^k \mid y^*) = \begin{cases} \min\left(\dfrac{p(y^*)\, q(y^k \mid y^*)}{p(y^k)\, q(y^* \mid y^k)}\right), & \text{if } p(y^k)\, q(y^* \mid y^k) > 0, \\ 1, & \text{otherwise.} \end{cases} \tag{14}$$

if rejected, then the current state is considered as the next state in the Markov chain. The full algorithm is described as below.

1. Set initial values $y^0 = (y_1^0, y_2^0, \ldots, y_k^0)$.
2. Repeat the following steps for $k(= 1, \ldots, n)$ iterations:
   - Create a proposal from $y^* \sim q(y^* \mid y^k)$.
   - Consider
   $$y^{(k+1)} = \begin{cases} y^*, & \text{if Unif}(0,1) \le \alpha(y^k \mid y^*), \\ y^k, & \text{Otherwise.} \end{cases}$$
3. Return the values $(y^0, \ldots, y^n)$.

The M-H method pays a lot in selecting a proposal distribution that is application-specific. Hastings (1970) proposed an alternative family of proposal distributions to Random-walk, say $q(y^*, y) = q(z)$, often known as independence M-H (IM), because the proposal is generated independently of the current value y^k. To make this idea work and avoid getting stuck in the tails of $p(\cdot)$, $q(z)$ must have thicker tails than $p(\cdot)$ [21]. In this study, the IM proposal distribution was selected as a Normal distribution centered at the current value with scale tuned to achieve acceptance rates around 0.25–0.35, as recommended for efficient mixing.

Reliable optimization processes to optimize the log-likelihood function are available in several statistical software. The computation in this paper is done using the R language [36]. For optimization, we created R code utilizing the `LaplaceApproximation` and `LaplacesDemon` functions from the package `LaplacesDemon`[40]. Furthermore, we created R code that uses the `jags` function to fit the model in JAGS. JAGS[33] is an intelligent open-source program for performing Bayesian inference using MCMC methods. JAGS employs a combination of Metropolis and Gibbs sampling, as well as additional MCMC techniques. In this instance, the JAGS program is finished using its R interface with the help of the `R2jags`[41] and `rjags`[35] packages.

In this study, the `LaplaceApproximation` was implemented using 5,000 iterations with a default burn-in of 500 iterations. For the `LaplacesDemon` approach, 40,000 iterations were used, with the first 10,000 discarded as burn-in. Similarly, the JAGS-based MCMC sampling was performed using 10,000 iterations, employing its default burn-in of 2,000 iterations. These settings were chosen to ensure stable posterior estimates and convergence across all approximation methods. Custom R code was written using these functions to compute these approximations, and the details are provided in the Appendix.

6. Model Compatibility

Model checks are crucial to modelling and analysis of statistical data. The Bayesian prior-to-posterior inferences presume the entire design of a probabilistic model and can draw the ambiguous or misleading conclusion if the model is poorly formulated. Therefore, at least some inspection of the adequacy of the model in relation to the data and the plausibility of the model for the purposes for which the model would be used should be included in a good Bayesian analysis[16]. This section assesses the adequacy of the fitted model through posterior predictive checks, including Bayesian p-values, which serve as an overall goodness-of-fit measure under the adopted criterion of fit[33].

6.1. Posterior Predictive checks and Bayesian p-value

In Bayesian theory, a usual way of assessment of model adequacy is the posterior predictive checks, specially when using MCMC methods of model fitting[16][17]. The basic principle of the posterior predictive checks is to compare the model's fit to observed data with its fit to replicated data generated from the posterior, which can also be represented graphically, called graphical posterior predictive checks. A typical feature of a good-fitting model is that about 50% of the observed data points lie above, and 50% lie below, the 1:1 line when compared to replicated values.

A quantitative summary is provided by the Bayesian p-value, which estimates the proportion of times the discrepancy measure under replicated data exceeds that under observed data. Values of the Bayesian p-value close to 0.5 indicate strong model adequacy, while values near 0 or 1 suggest a poor fit. In Bayesian applications, these p-values are not classical significance tests but reflect how often posterior-replicated datasets produce larger discrepancies than the observed dataset.

In this study, both the graphical checks and the numerical Bayesian p-values were computed using replicated samples generated directly from the MCMC posterior draws. For both our datasets, the values remained near 0.5, indicating that the expRay model provides an adequate fit to the survival patterns observed in the IUD and bladder cancer data.

7. Simulation Study

To strengthen the empirical evidence and objectively evaluate estimator performance, a Monte Carlo simulation study was conducted to examine the performance of frequentist and Bayesian behavior of the Exponentiated Rayleigh (expRay) regression model under right-censoring. Specifically, we compared (i) Maximum Likelihood Estimation (MLE) and (ii) Bayesian inference implemented in Stan across varying sample sizes and censoring levels. This controlled design complements the real-data analyses and quantifies estimator accuracy and stability using bias, root-mean-square error (RMSE), and coverage probability. All simulations were implemented in R (4.4.1) using Stan (2.35) via the `rstan` package[46]. Reproducible code and random-seed values are provided in Appendix B.

7.1. Data-Generating Mechanism

For subject i, survival times T_i were generated from the expRay distribution with shape parameter $a > 0$ and scale parameter $\lambda_i > 0$:

$$F(t \mid a, \lambda_i) = \left(1 - e^{-(t/\lambda_i)^2}\right)^a, \quad t > 0.$$

The scale parameter was linked to a set of covariates $X_i = (1, X_{i1}, \ldots, X_{ip})^\top$ through the log-linear predictor

$$\log(\lambda_i) = X_i^\top \beta$$

with regression coefficient vector β. Event times were generated via the inverse-transform method,

$$T_i = \lambda_i \sqrt{-\log\left(1 - U_i^{1/a}\right)}, \quad U_i \sim \text{Uniform}(0, 1).$$

To mimic incomplete follow-up, independent right censoring was introduced. Censoring times C_i were drawn from an exponential distribution with rate parameter chosen to yield an average censoring proportion of approximately 25%. The observed time was defined as $Y_i = \min(T_i, C_i)$ with event indicator $\delta_i = I(T_i \leq C_i)$.

7.2. Simulation Design

Two designs were considered:

- **Two-parameter model.** Datasets of size $n = 100, 300, 500$ were generated with a single covariate $X_{i1} \sim N(0, 1)$. Parameters were fixed at $\beta = (0.5, -0.8)$ and $a = 0.7$, representing moderate effects and a departure from the Rayleigh special case $(a = 1)$.
- **Three-parameter model.** Datasets of size $n = 100, 300, 500$ were generated with two covariates, $X_{i1} \sim N(0, 1)$ and $X_{i2} \sim$ Bernoulli(0.5). Parameters were fixed at $\beta = (1.0, -0.5, 0.3)$ and $a = 1.2$, to examine mixed covariate types and a heavier-tailed distribution.

7.3. Estimation Methods

For each dataset, two estimation procedures were applied:

- **Maximum Likelihood Estimation (MLE):** Parameter estimates were obtained by numerically maximizing the log-likelihood using the `optim` routine in R. Standard errors were derived from the observed information matrix. In several small-sample, moderately censored datasets the Hessian failed to converge, producing unstable standard errors—an issue expected for non-linear survival models with shape parameters.
- **Bayesian Estimation (via Stan):** A Bayesian expRay regression model was implemented in Stan. WIPs were assigned, specifically $\beta_j \sim$ Normal$(0, 5)$ and $\log a \sim$ Normal$(0, 2)$. Posterior inference was based on four parallel Markov chains each with 2000 iterations and discarding the first 1000 as burn-in. Convergence was confirmed with $\hat{R} < 1.01$ and effective sample sizes (ESS) > 1500 for all parameters. These settings produced stable posterior summaries across all scenarios.

7.4. Performance Measures

Across 100 Monte Carlo replications for both parameter settings, the following metrics were computed for each estimation approach:

- **Bias:** the difference between the average estimate and the true parameter.
- **Root Mean Square Error (RMSE):** a measure of overall accuracy.
- **Coverage Probability:** the proportion of 95% confidence intervals (for MLE) or 95% credible intervals (for Bayesian inference) containing the true value.
- **Posterior summaries:** posterior means, standard deviations, and credible intervals for Bayesian estimation.
- **Computation time:** Average computation times (MLE vs. Bayesian sampling) were also recorded to evaluate computational efficiency.

This simulation design allows us to assess both the frequentist and Bayesian properties of the proposed expRay regression model under realistic sample sizes and moderate censoring levels.

7.5. Results

Tables 1 and 2 summarize results for the two- and three-parameter models, respectively. Both MLE and Bayesian procedures were approximately unbiased, with RMSE decreasing as n increased. Bayesian credible intervals were generally narrower yet maintained coverage close to nominal levels.

For small samples, the MLE occasionally failed to converge under moderate censoring, resulting to inflated RMSE and occasional coverage deficiencies. In contrast, the Bayesian approach consistently yielded accurate point estimates with negligible bias and robust coverage.

Computation times averaged 0.9 s (MLE) and 1.4 s (Bayesian–Stan) per dataset of $n = 500$. The Bayesian method achieved higher sampling efficiency, with ESS/time ratios approximately three times greater than for MLE resampling.

Table 1. Simulation results for the expRay regression model with true values $\beta_0 = 0.50$, $\beta_1 = -0.8$, $a = 0.70$. Estimates are averages across 100 Monte Carlo replications under 25% censoring. Bias, RMSE, and coverage refer to 95% confidence (MLE) or credible (Bayes) intervals.

n	Parameter	True Value	Method	Estimate (SE/SD)	Bias	RMSE	Coverage
100	β_0	0.50	MLE	0.469 (0.123)	0.005	0.104	1.00
			Bayes	0.496 (0.122)	0.033	0.111	1.00
	β_1	-0.80	MLE	-0.837 (0.094)	-0.031	0.087	0.94
			Bayes	-0.839 (0.094)	-0.034	0.088	0.94
	a	0.70	MLE	0.731 (0.146)	0.018	0.114	0.98
			Bayes	0.719 (0.102)	0.008	0.111	0.92
300	β_0	0.50	MLE	0.521 (0.064)	-0.020	0.065	0.96
			Bayes	0.528 (0.063)	-0.011	0.064	0.96
	β_1	-0.80	MLE	-0.853 (0.056)	0.006	0.050	0.96
			Bayes	-0.851 (0.056)	0.005	0.051	0.94
	a	0.70	MLE	0.652 (0.079)	0.024	0.068	0.99
			Bayes	0.649 (0.051)	0.020	0.067	0.96
500	β_0	0.50	MLE	0.468 (0.049)	-0.005	0.049	0.94
			Bayes	0.473 (0.050)	0.001	0.049	0.94
	β_1	-0.80	MLE	-0.766 (0.040)	0.003	0.046	0.90
			Bayes	-0.766 (0.042)	0.002	0.046	0.90
	a	0.70	MLE	0.744 (0.064)	0.015	0.041	0.99
			Bayes	0.742 (0.047)	0.012	0.040	1.00

7.6. Findings from the Simulation Study

The simulation study confirmed that both frequentist and Bayesian procedures can recover the true parameters of the expRay regression model. However, Bayesian estimation consistently resulted more stable inference, with smaller RMSE and reliable coverage in all scenarios. In contrast, MLE was more sensitive to censoring and occasionally failed to converge in smaller samples. Larger sample sizes improved precision for both methods.

Overall, the results reinforce the robustness of the Bayesian framework for practical applications of the expRay model to right-censored survival data. In the subsequent real-data analyses, Bayesian estimation is therefore used as the primary inference method.

8. Application with Real Data Sets

This section presents the application of the exponentiated Rayleigh (expRay) regression model to two right-censored survival datasets: (i) the Intra-Uterine Device (IUD) discontinuation data and (ii) the bladder cancer remission data. For both datasets, classical MLE and Bayesian methods (Laplace Approximation, Independent Metropolis, and JAGS) were applied exactly as described in Sections 4–5. Model adequacy was assessed using posterior predictive checks and Bayesian p-values (Section 6).

8.1. Intra-Uterine Device Data Set

The IUD dataset, originally collected by the World Health Organization [47] and later discussed in Collett [9], contains the number of weeks from insertion of a Multiload-250 intra-uterine device to discontinuation due to

Table 2. Simulation results for the expRay regression model with true values ($\beta_0 = 1.0, \beta_1 = -0.5, \beta_2 = 0.3, a = 1.2$). Estimates are averages across 100 Monte Carlo replications under 25% censoring. Bias, RMSE, and coverage refer to 95% confidence (MLE) or credible (Bayesian) intervals.

n	Parameter	True Value	Method	Estimate (SE/SD)	Bias	RMSE	Coverage
100	β_0	1.0	MLE	1.059 (0.103)	0.170	0.774	0.90
			Bayes	1.087 (0.106)	0.018	0.106	0.94
	β_1	-0.5	MLE	-0.420 (0.070)	-0.054	0.596	–
			Bayes	-0.423 (0.072)	-0.003	0.075	0.94
	β_2	0.3	MLE	0.398 (0.121)	0.624	2.640	0.90
			Bayes	0.394 (0.126)	0.002	0.123	0.94
	a	1.2	MLE	1.076 (0.152)	-0.046	0.340	0.82
			Bayes	1.051 (0.159)	-0.012	0.190	0.92
300	β_0	1.0	MLE	0.887 (0.057)	0.121	0.936	0.92
			Bayes	0.895 (0.056)	-0.003	0.051	0.96
	β_1	-0.5	MLE	-0.458 (0.035)	-0.054	0.359	–
			Bayes	-0.459 (0.035)	-0.004	0.033	0.98
	β_2	0.3	MLE	0.387 (0.066)	0.132	0.970	0.94
			Bayes	0.387 (0.066)	-0.002	0.075	0.96
	a	1.2	MLE	1.293 (0.091)	0.001	0.191	0.90
			Bayes	1.283 (0.117)	0.014	0.102	1.00
500	β_0	1.0	MLE	0.996 (0.046)	-0.002	0.051	0.92
			Bayes	1.002 (0.047)	0.003	0.051	0.92
	β_1	-0.5	MLE	-0.482 (0.029)	0.005	0.029	0.98
			Bayes	-0.482 (0.029)	0.005	0.029	0.98
	β_2	0.3	MLE	0.254 (0.055)	0.000	0.063	0.90
			Bayes	0.255 (0.055)	0.001	0.064	0.90
	a	1.2	MLE	1.213 (0.071)	0.010	0.092	0.90
			Bayes	1.205 (0.086)	0.002	0.0901	0.92

menstrual bleeding complications. Eighteen women aged 18–35 were followed, all having two prior pregnancies. Although the study was designed for two-year follow-up, three observations were right-censored due to withdrawal for unrelated reasons (e.g., desire for pregnancy or loss to follow-up).

Table 3 lists the discontinuation times (with * indicating censoring). A Kaplan–Meier survival curve as shown in Figure 2, illustrates the decreasing probability of continued device use over time and marking censored observations via vertical ticks.

Table 3. Times in weeks to discontinuation of the use of an IUD.

10	13*	18*	19	23*	30	36	38*	54*
56*	59	75	93	97	104*	107	107	107*

8.2. Bladder Cancer Data Set

The second dataset (Table 4) contains remission times for 137 bladder cancer patients, originally compiled in Lee and Wang [19] and later it was re-analyzed using extended Weibull models by Klakattawi [18]. The dataset includes both observed relapse times and right-censored observations, indicated by asterisk (*). Figure 3 shows the Kaplan–Meier survival curve, which reflects a steady decline in remission probability over time, with higher relapse risk early in follow-up.

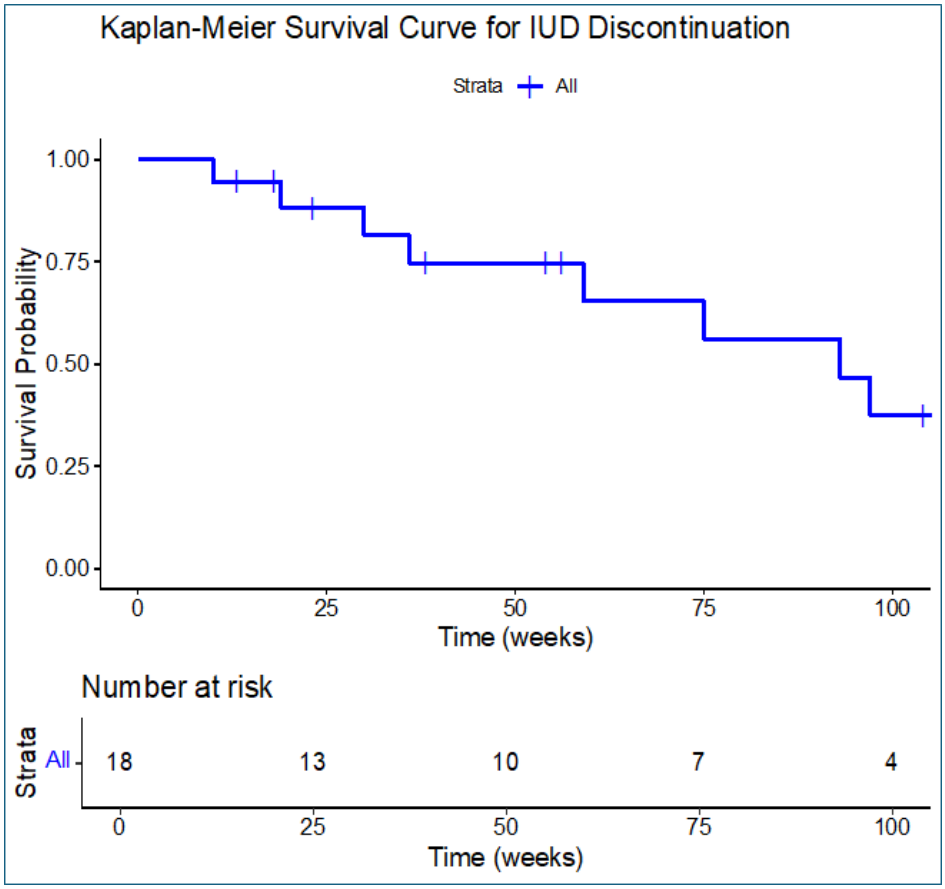

Figure 2. Kaplan–Meier survival curve illustrating the probability of continued IUD use over time among 18 women. The stepwise curve reflects observed discontinuation events, while vertical tick marks indicate right-censored observations. The risk table below shows the number of women still at risk at key time points.

Table 4. Remission times (in months) of bladder cancer patients.

0.08	2.09	3.48	4.87	6.94	8.66	13.11	23.63	0.20	2.23	3.52	4.98
6.97	9.02	13.29	24.80*	0.40	2.26	3.57	5.06	7.09	9.22	13.80	25.74
0.50	2.46	3.64	5.09	7.26	9.47	14.24	25.82	0.51	2.54	3.70	5.17
7.28	9.74	14.76	26.31	0.81	2.62	3.82	5.32	7.32	10.06	14.77	32.15
0.87*	2.64	3.88	5.32	7.39	10.34	14.83	34.26	0.90	2.69	4.18	5.34
7.59	10.66	15.96	36.66	1.05	2.69	4.23	5.41	7.62	10.75	16.62	43.01
1.19	2.75	4.26	5.41	7.63	10.86*	17.12	46.12	1.26	2.83	4.33*	5.49
7.66	11.25	17.14	79.05	1.35	2.87	4.33	5.62	7.87	11.64	17.36	1.40
3.02*	4.34	5.71	7.93	11.79	18.10	1.46	3.02	4.40	5.85	8.26	11.98
19.13	1.76	3.25	4.50	6.25	8.37	12.02	19.36*	2.02	3.31	4.51	6.54
8.53	12.03	20.28	2.02	3.36	4.65*	6.76	8.60*	12.07	21.73	2.07	3.36
4.70*	6.93	8.65	12.63	22.69							

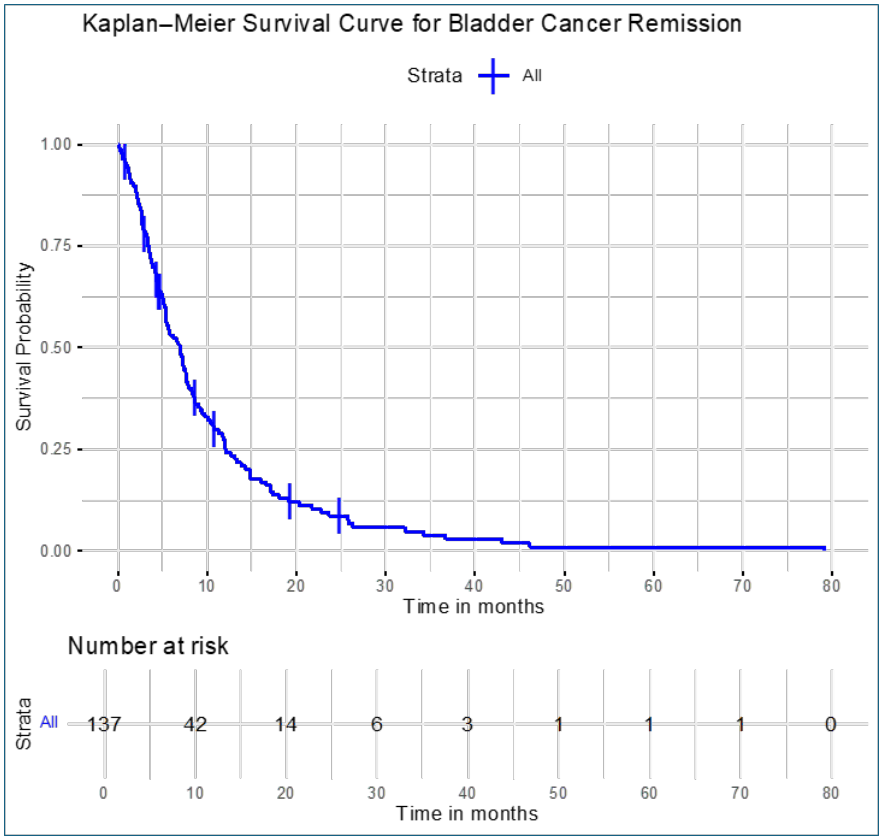

Figure 3. Kaplan–Meier survival curve showing estimated probability of remaining in remission for 137 bladder cancer patients. Vertical ticks represent right-censored observations. The risk table indicates the number of patients remaining at risk at each interval.

9. Implementation and Results

For both datasets, the expRay model

$$y_i \sim \text{expRay}(a, \lambda_i) \quad \log(\lambda_i) = X_i\beta,$$

was fitted using both frequentist and Bayesian methods. The prior distributions were:

$$\beta_j \sim \text{Normal}(0, 1000), \quad a \sim \text{Half-Cauchy}(25),$$

consistent with the weakly informative priors specified in Section 4.2. For JAGS, a Uniform prior $a \sim \text{Uniform}(0, 10)$ was used to allow Poisson zeros-trick implementation and to assess prior sensitivity.

Initial values for Laplace Approximation and IM estimation were chosen via a simple regression of $\log(y)$ on an intercept, which improved convergence stability. Posterior predictive checks were performed following the procedure in Section 6. Bayesian p-values near 0.5 indicated satisfactory model fit for both datasets.

9.1. Results for finding for IUD Data

Both Maximum Likelihood Estimation (MLE) and Bayesian Estimation techniques provided important observations relating to the parameter estimation for the model in concern.

Maximum Likelihood Estimation The MLE results, presented in Table 5, were notably uniform across all three optimization algorithms. Parameters β were estimated using the Nelder-Mead, Conjugate-Gradients, and L-BFGS-B methods and so were 4.70, SE = 0.27, log.a was also estimated as -0.26, SE = 0.35. By excluding zero, the 95% CIs for β, which varied from 4.16 to 5.24, indicated statistical significance. Nonetheless, the log.a interval (-0.95 to 0.43) did contain zero, indicating that this parameter might not be statistically significant at conventional levels. This consistency across optimization methods may underscore the reliability of the MLE approach for the IUD dataset. Given that these results seem to align with the logic of the problem, it can more accurate be suggested that optimization methodology does not have considerable effect on parameter captures influencing the noted outcomes, therefore proving the dependability of the MLE optimization model.

Table 5. Maximum likelihood estimates for exponentiated Rayleigh model parameters showing consistent results across all three optimization algorithms for the IUD dataset (N=18).

	Maximum-Likelihood Estimation											
	Nelder-Mead Method				Conjugate-Gradients Method				L-BFGS-B Method			
Parameter	Mean	SE	LB	UB	Mean	SE	LB	UB	Mean	SE	LB	UB
Beta	4.70	0.27	4.16	5.24	4.70	0.27	4.16	5.24	4.70	0.27	4.16	5.24
log.a	-0.26	0.35	-0.95	0.42	-0.26	0.35	-0.95	0.43	-0.26	0.35	-0.95	0.43

Bayesian Estimation The Bayesian analysis synthesized the uncertainty at the parameters through posterior distributions in a better way. The Laplace Approximation yielded posterior means of $\beta = 4.85$ (SD=0.33) and $a = 0.73$ (SD=0.26), with a deviance of 102.76. The Independent Metropolis (IM) algorithm gave a tighter estimate of $\beta = 4.71$ (SD=0.11) and $a = 0.78$ (SD=0.12) parameters, with the lowest deviance (100.92), suggesting the overall best performance. The JAGS implementation yielded intermediate estimates $\beta = 4.75$ (SD=0.29) and $a = 0.83$ (SD=0.28), with a deviance of (102.54). Notably, the IM algorithm showed superior performance in terms of precision, as evidenced by narrower credible intervals and lower deviance values. These findings are also demonstrated in the accompanying plots.

Table 6. Posterior summaries for Bayesian parameter estimates of the expRay (β, a) model using three computational approaches (IUD data, N = 18). Results show posterior means with standard deviations (SD), along with 2.5% (LB), 50% (Median), and 97.5% (UB) credible intervals, deviance statistics, and log-posterior (LP) values for the IUD discontinuation dataset $(N = 18)$. The IM algorithm demonstrated optimal performance with the lowest deviance (100.92) and narrowest credible intervals.

	Bayesian Estimation											
	Laplace Approximation				Independent-Metropolis Algorithm				JAGS Method			
Parameter	Mean	SD	LB	UB	Mean	SD	LB	UB	Mean	SD	LB	UB
Beta	4.85	0.33	4.30	5.58	4.71	0.11	4.50	4.95	4.75	0.29	4.27	5.43
log.a	-0.38	0.36	-1.14	0.29	-0.26	0.15	-0.56	0.02	-	-	-	-
Deviance	102.76	2.07	100.66	107.78	100.92	0.37	100.58	101.80	102.54	1.94	100.61	107.85
a	0.73	0.26	0.32	1.33	0.78	0.12	0.57	1.02	0.73	0.28	0.39	1.49

Figures 5 illustrate the posterior distributions and trace plots for the Bayesian estimates. These diagnostic assessments provided further validation of our results. Trace plots as shown in this figure demonstrated excellent convergence properties for all Bayesian methods, with the IM algorithm showing particularly stable mixing. Posterior predictive checks yielded a Bayesian p-value of 0.54, close to the ideal value of 0.5, indicating good model fit. The shape parameter estimates $(a \approx 0.7 - 0.8)$ suggested a moderately increasing hazard function for IUD discontinuation times. The posterior predictive plots (see Figure 6) illustrate the density of simulated values for the fitted responses $\hat{y}_i$ for selected observations (1—18), with red vertical lines marking the actual observed outcomes. These plots provide a visual assessment of model fit by comparing observed values to the distribution of replicated data generated from the posterior. When the observed value (red line) falls near the center of the density curve, it indicates a good fit for that observation, while placement in the tails may suggest poor fit or a potential

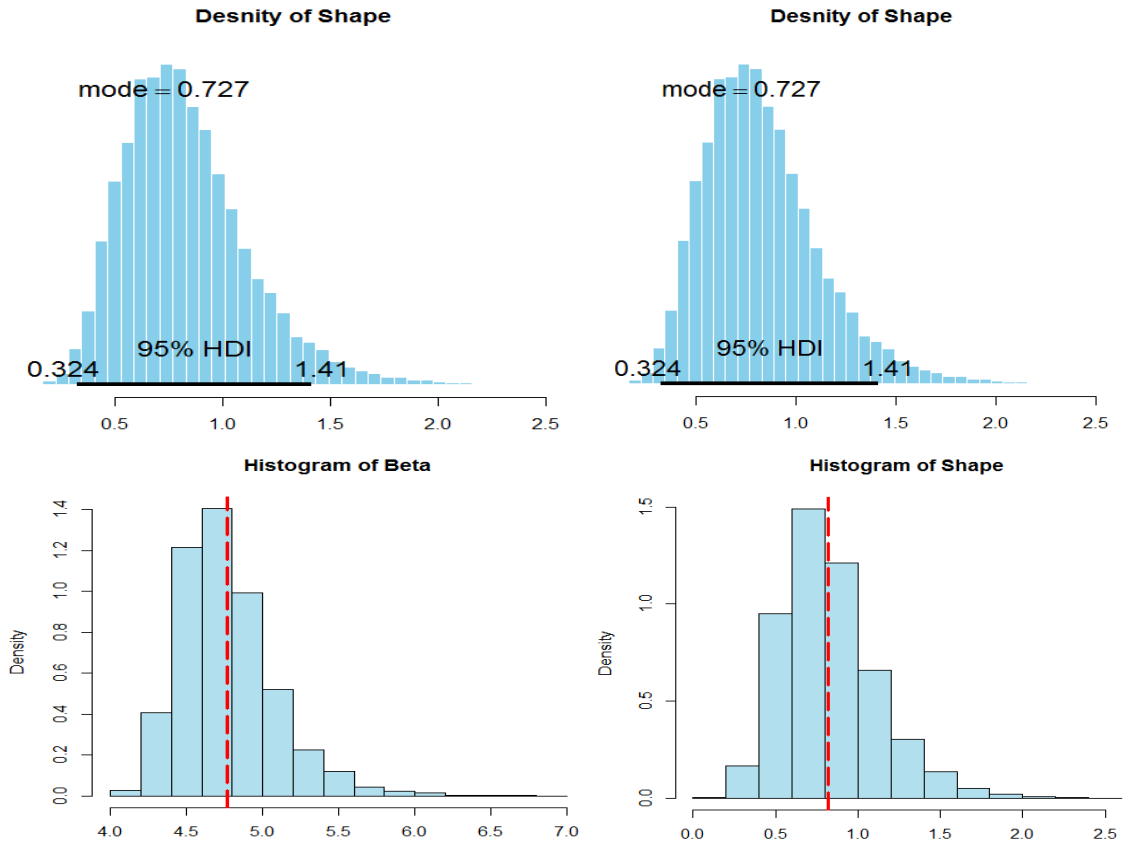

Figure 4. Posterior density plots and histograms of beta (β) and shape parameter (a) estimates using JAGS, showing posterior distributions with mode and 95% highest posterior density intervals, demonstrating parameter uncertainty in the exponentiated Rayleigh modes (IUD discontinuation dataset, $N = 18$.

outlier. In this case, most of the red lines lie within high-density regions, implying that the model accurately captures the underlying data-generating process. This visual alignment further supports the posterior predictive p-value near 0.5, confirming the adequacy of the model.

This comparative assessment revealed that while all methods produced substantively similar results, the IM algorithm offered the best balance between computational efficiency and statistical precision for this dataset (e.g., Figure 7). The Laplace approximation, while fastest, tended to produce slightly inflated estimates, while JAGS, though flexible, was more computationally intensive without offering clear advantages in model fit for this particular application.

These findings highlight the robustness of the exponentiated Rayleigh model and demonstrate the utility of Bayesian methods, especially IM, in survival analysis of small, right-censored datasets like this one.

Figure 8 shows the estimated survival probabilities over time (in weeks) for women using the IUD, derived from the posterior distributions of the Exponentiated Rayleigh model fitted via three Bayesian methods. Each line represents the posterior mean survival curve from one method, while the shaded regions represent the 95% credible intervals. The curves from all three methods (JAGS in red, IM in green, LA in blue) follow a similar declining trend, indicating consistent estimates of decreasing survival probability (i.e., higher risk of discontinuation over time). Slight differences in the width of the shaded areas reflect each method's uncertainty quantification–with IM

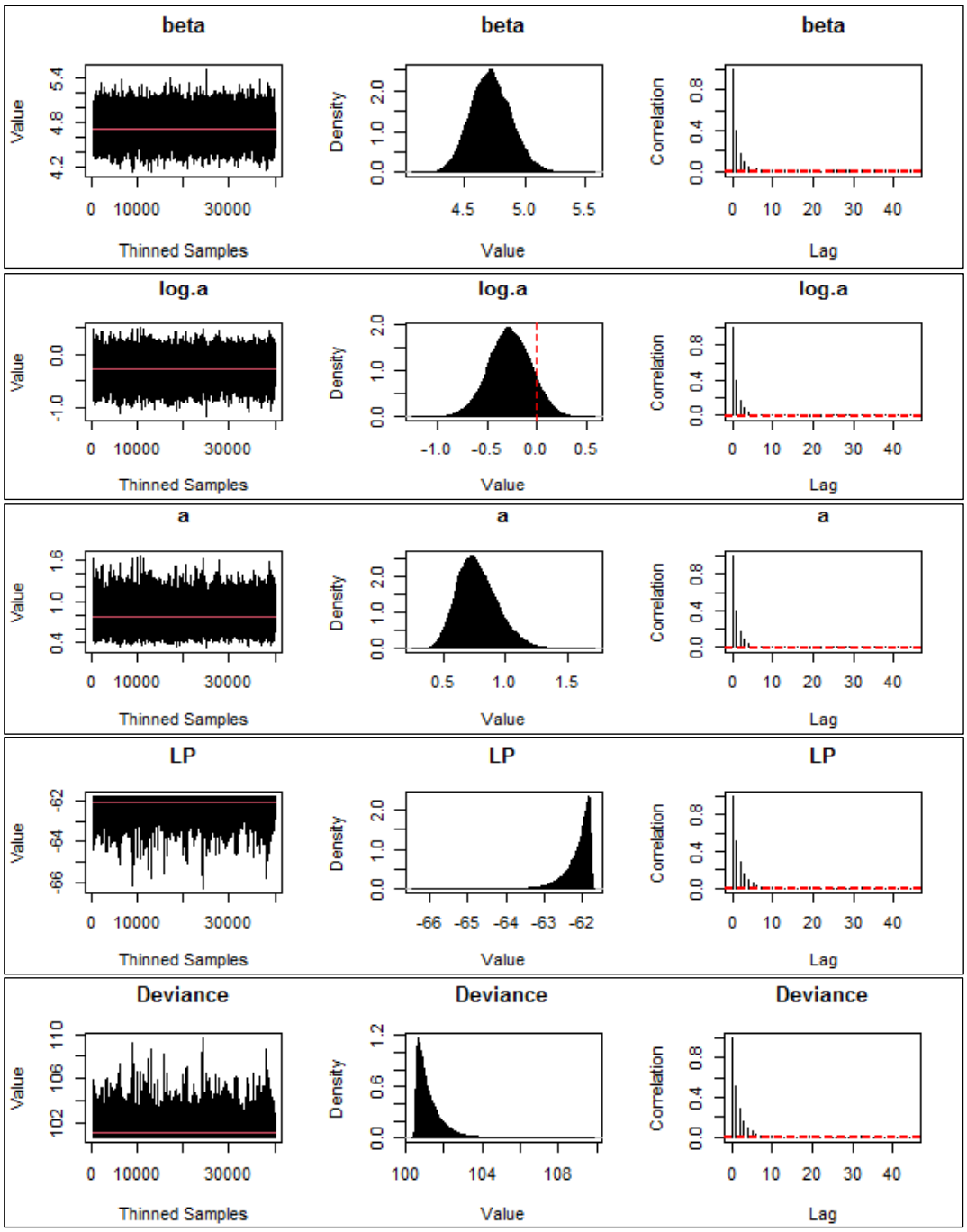

Figure 5. Trace plot diagnostics demonstrating convergence of Markov chains for three Bayesian estimation methods, showing successful mixing and stationarity for all exponentiated Rayleigh model parameters ($\hat{R} < 1.01$) (IUD discontinuation dataset, $N = 18$).

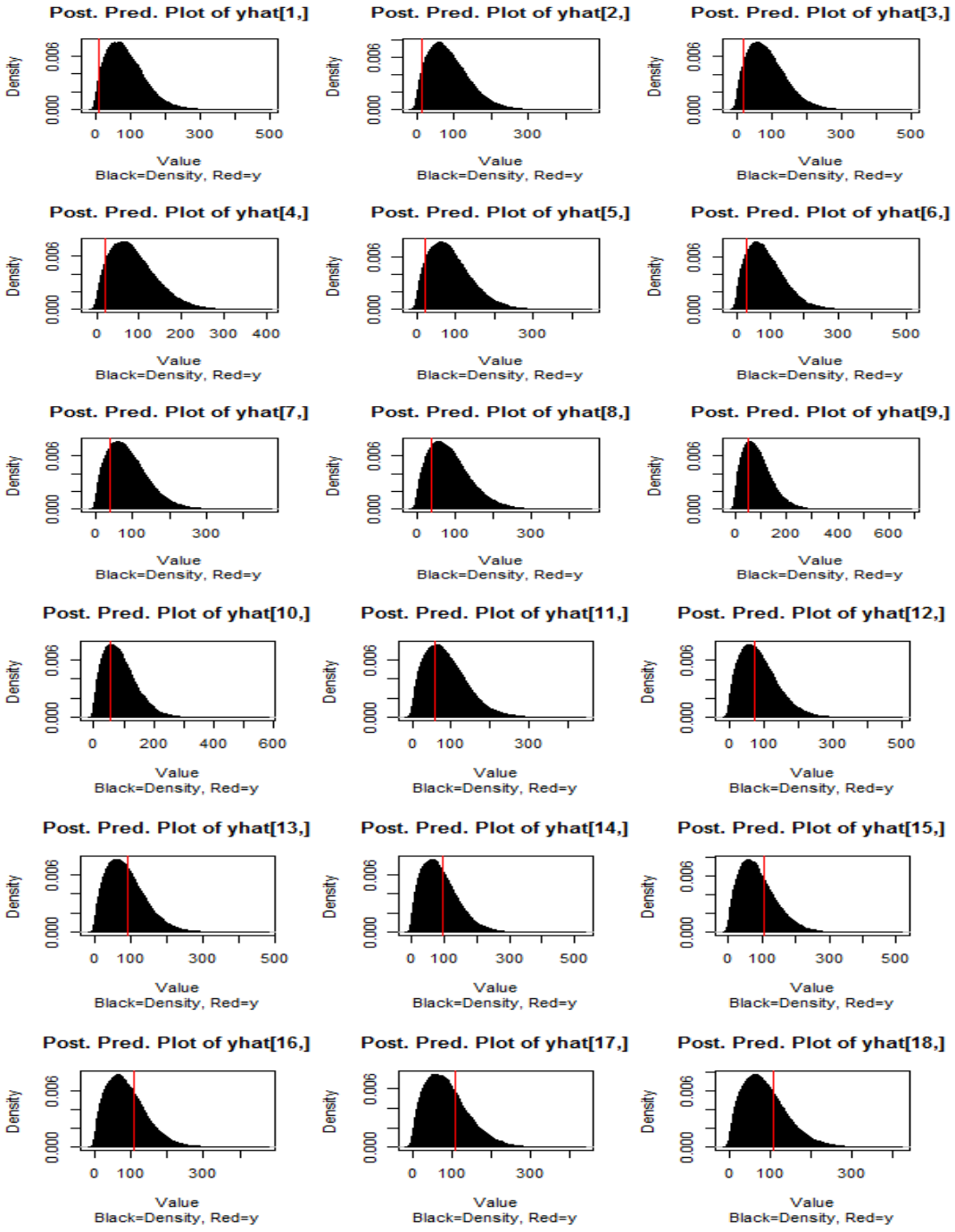

Figure 6. Posterior predictive density plots for fitted values $\hat{y}_i$ (observations 1–18), showing the model's ability to reproduce observed data; red lines indicate observed values, with alignment to high-density regions suggesting good model fit (IUD discontinuation dataset, $N = 18$).

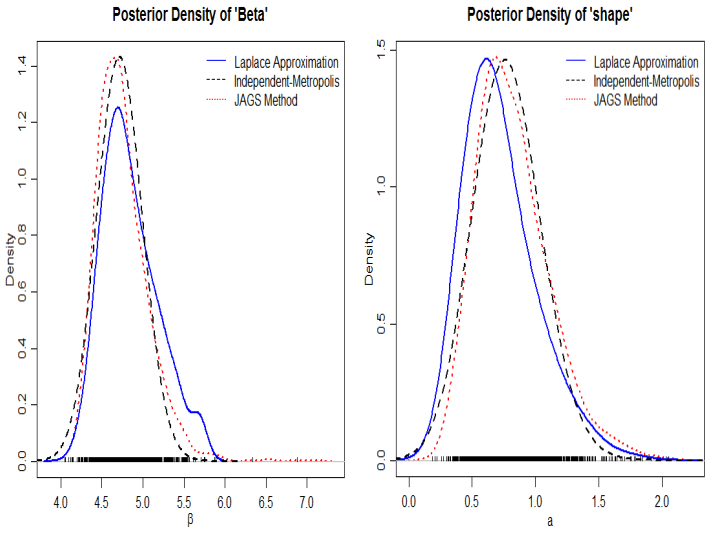

Figure 7. Posterior density for β parameter (left) and shape parameter a (right) estimated via Laplace Approximation (solid line, blue), Independent Metropolis (dashed line, green), and JAGS (dotted line, red) methods (IUD discontinuation dataset, $N = 18$).

producing narrower credible intervals than JAGS followed by LA. This consistency affirms the model's robustness and the comparability of inference across Bayesian estimation techniques.

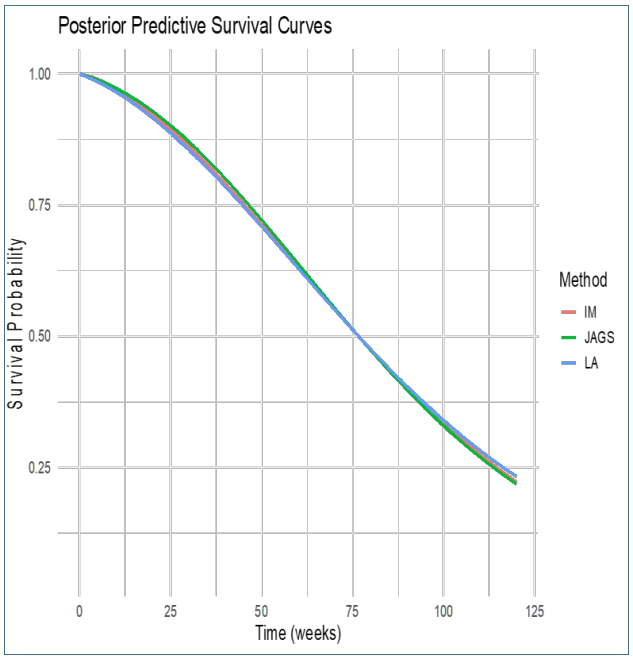

Figure 8. Posterior predictive survival curves for the IUD discontinuation data (N=18) using the Exponentiated Rayleigh model fitted via Laplace Approximation (blue), Independence Metropolis (green), and JAGS (red). Shaded areas indicate 95% credible intervals.

9.2. Results for finding for Bladder Data

The analysis of the bladder cancer remission data revealed important insights through both maximum likelihood and Bayesian estimation approaches.

Maximum Likelihood Estimation: The maximum likelihood estimation demonstrated strong consistency across optimization methods, with identical estimates obtained from all three Nelder-Mead, Conjugate-Gradients, and L-BFGS-B algorithms, underscoring numerical stability. The regression coefficient was estimated as $\beta = 3.07$ (SE = 0.08) with a 95% confidence interval of [2.91, 3.24], indicating statistically significant effects. The value of log.a = -0.99 (SE = 0.10) which indicates $a \approx 0.37$, suggests a hazard function that declines with time, which aligns well with clinical expectations regarding cancer remission patterns. The confidence interval of these MLE results received from different optimization approaches that converged was constructive.

Table 7. MLE results using three optimization algorithms for bladder cancer remission data (N = 137).

	Maximum-Likelihood Estimation											
	Nelder-Mead Method				Conjugate-Gradients Method				L-BFGS-B Method			
Parameter	Mean	SE	LB	UB	Mean	SE	LB	UB	Mean	SE	LB	UB
Beta	3.07	0.08	2.91	3.24	3.07	0.08	2.91	3.24	3.07	0.08	2.91	3.24
log.a	-0.99	0.10	-1.18	-0.79	-0.99	0.10	-1.18	-0.79	-0.99	0.10	-1.18	-0.79

Bayesian Estimation: Further, using three separate computational techniques – Laplace Approximation, Independent-Metropolis (IM), and JAGS, Bayesian analysis provided deeper insights into parameter uncertainty. While all methods produced similar posterior means, JAGS consumed more resources whereas the IM approach yielded the most precise estimates with the narrowest credible intervals and the lowest deviance (873.14). Posterior means of β ranged from 3.08 to 3.09, and for a, from 0.37 to 0.38, further confirming the downward trend in hazard over time. Notably, the IM algorithm achieved strong convergence and sampling efficiency, as evidenced by trace plots and effective sample sizes.

Table 8. Bayesian parameter estimates for the expRay model using Laplace, IM, and JAGS methods (bladder cancer data, N = 137).

	Bayesian Estimation														
	Laplace Approximation					Independent-Metropolis Algorithm					JAGS Method				
Parameter	Mean	SD	LB	Med	UB	Mean	SD	LB	Med	UB	Mean	SD	LB	Med	UB
Beta	3.09	0.08	2.94	3.08	3.25	3.08	0.05	2.98	3.07	3.17	3.08	0.08	2.92	3.08	3.24
log.a	-0.99	0.09	-1.17	-0.99	-0.89	-0.99	0.06	-1.10	-0.99	-0.87					
Deviance	874.20	1.65	872.49	873.71	878.37	873.14	0.71	872.45	872.92	875.04	874.45	1.94	872.49	873.83	879.74
LP	-448.60	0.82	-450.68	-448.35	-447.74	-448.07	0.35	-449.02	-447.96	-447.72					
a	0.37	0.04	0.31	0.37	0.45	0.37	0.02	0.33	0.37	0.42	0.38	0.04	0.31	0.38	0.45

Diagnostic assessments affirmed model adequacy. Trace plots exhibited stable convergence, with the IM algorithm yielding especially efficient sampling. Posterior predictive checks produced a Bayesian p-value of 0.52, indicating good model fit. The shape parameter estimates ($a \approx 0.37$) confirmed a declining hazard rate, aligning with clinical expectations.

Residual analyses showed no discernible patterns, supporting the suitability of the expRay model for this dataset. The consistency of findings across estimation methods enhanced confidence in the identified survival trends.

From a methodological standpoint, the IM algorithm provided the tightest credible intervals and lowest deviance. Laplace approximation was fastest but showed broader intervals, while JAGS was more computationally intensive without notable gains in model performance. While both MLE and Bayesian methods converged on the key insight of decreasing hazard, Bayesian estimation enriched inference by quantifying uncertainty more fully. IM's roughly 38% narrower credible intervals compared to Laplace emphasize its precision.

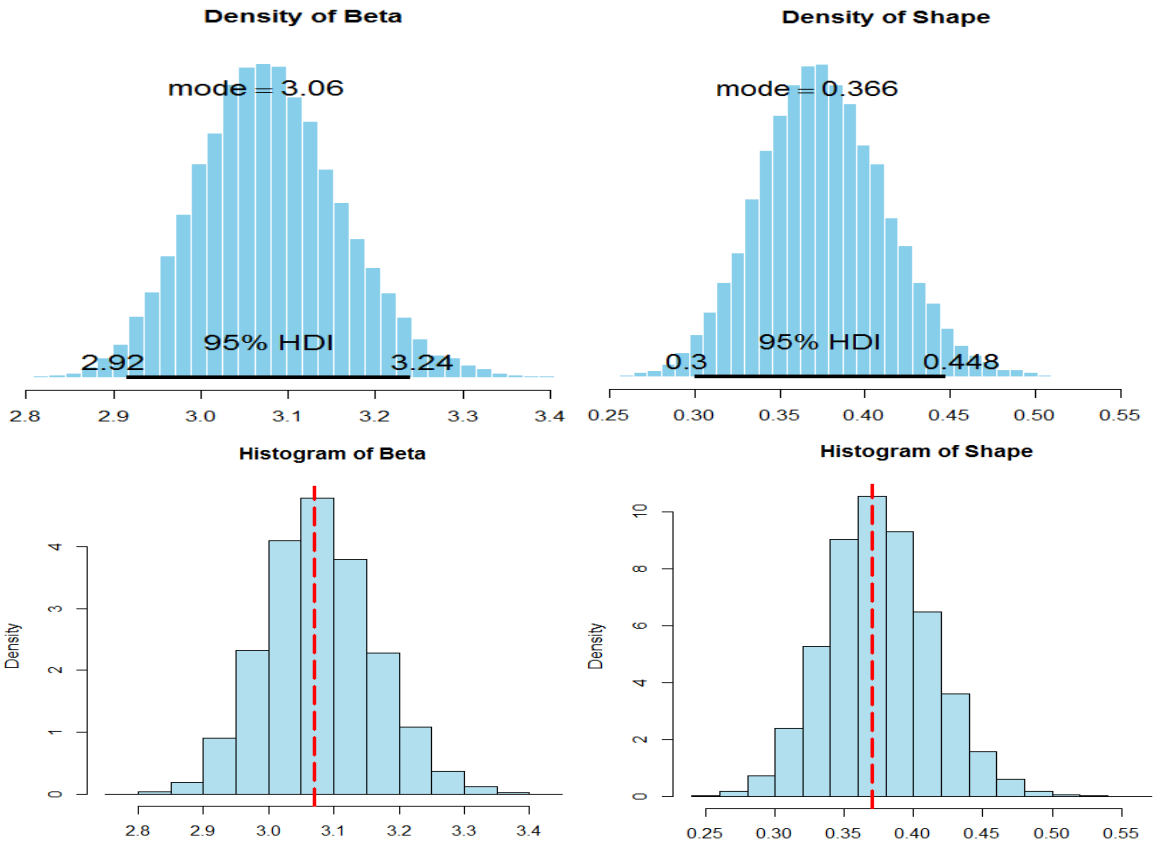

Figure 9. Posterior density plots and histograms of beta (β) and shape parameter (a) estimates using JAGS, showing posterior distributions with mode and 95% highest posterior density intervals, demonstrating parameter uncertainty in the exponentiated Rayleigh modes (Bladder cancer data, N = 137).

These results highlight the strength of combining classical and Bayesian methods for robust survival analysis. They confirm the declining hazard in cancer remission and demonstrate the exponentiated Rayleigh model's suitability for modeling such time-to-event data with censoring.

The posterior predictive plots for $\hat{y}_i$ $(i = 1\ to\ 18)$, shown in Figure 11, illustrate the model's performance by comparing predicted distributions (in black) with the actual observed values (red vertical lines). These plots are a crucial Bayesian diagnostic tool for checking the adequacy of the model's predictive performance. In most cases, the red lines fall within high-density regions of the posterior predictive distribution, indicating that the model captures the data-generating process effectively. Where observed values lie near the tails, potential model misfit or data irregularities may exist. Overall, the good alignment in most plots supports the reliability of the fitted exponentiated Rayleigh model for remission time predictions.

Furthermore, Figure 13 presents the posterior predictive survival curves for patients with bladder cancer, based on the exponentiated Rayleigh model estimated using three Bayesian methods: Laplace Approximation (LA), Independence Metropolis (IM), and JAGS. All three curves show a steep and rapid decline in survival probability early on, which is characteristic of a decreasing hazard function—implying that the risk of remission or event occurrence is highest soon after treatment and diminishes with time. The tight credible intervals across all methods indicate high estimation precision, with minimal divergence among the methods. This strong agreement across

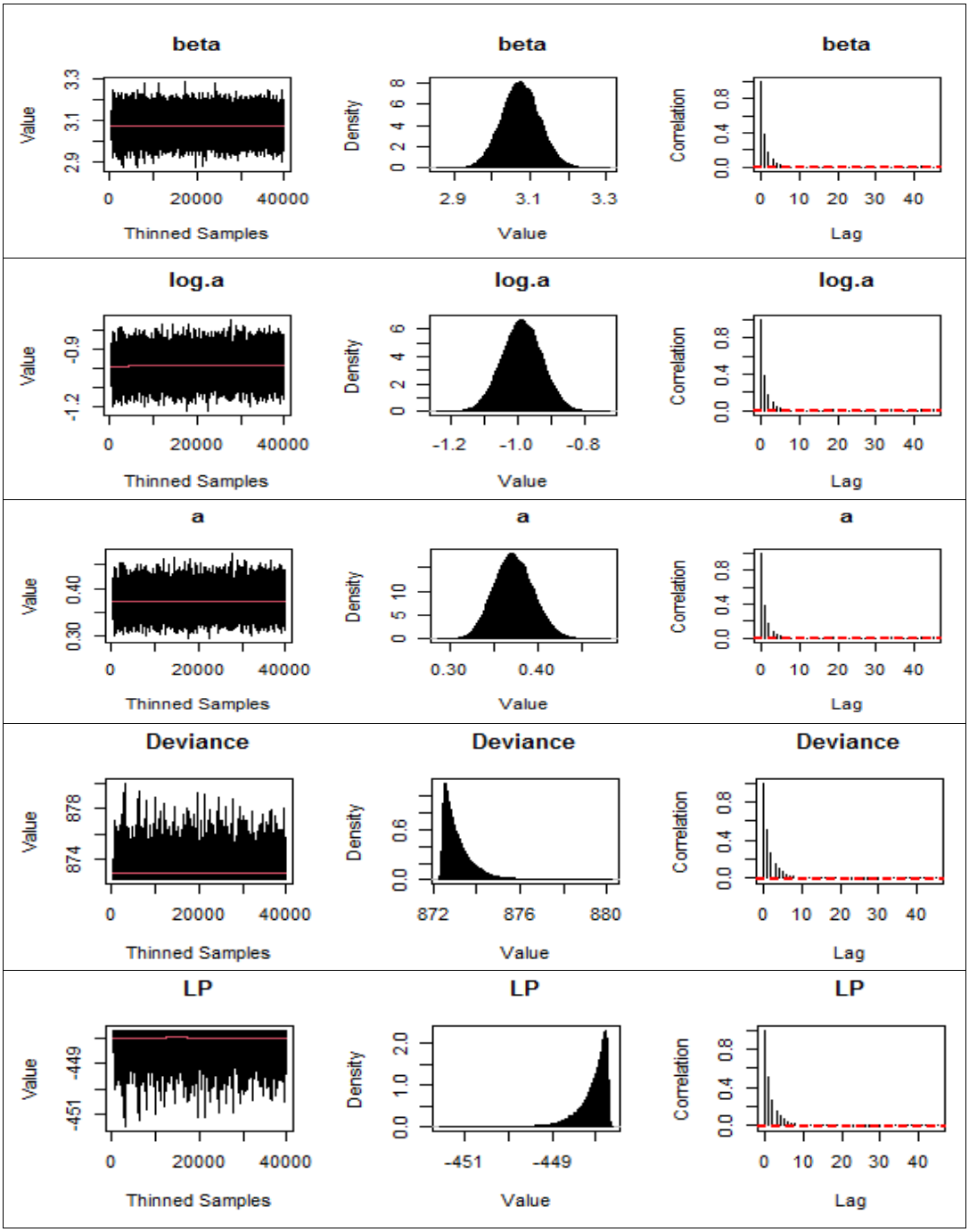

Figure 10. Trace plot diagnostics demonstrating convergence of Markov chains for three Bayesian estimation methods, showing successful mixing and stationarity for all exponentiated Rayleigh model parameters ($\hat{R} < 1.01$) (Bladder cancer data, $N = 137$).

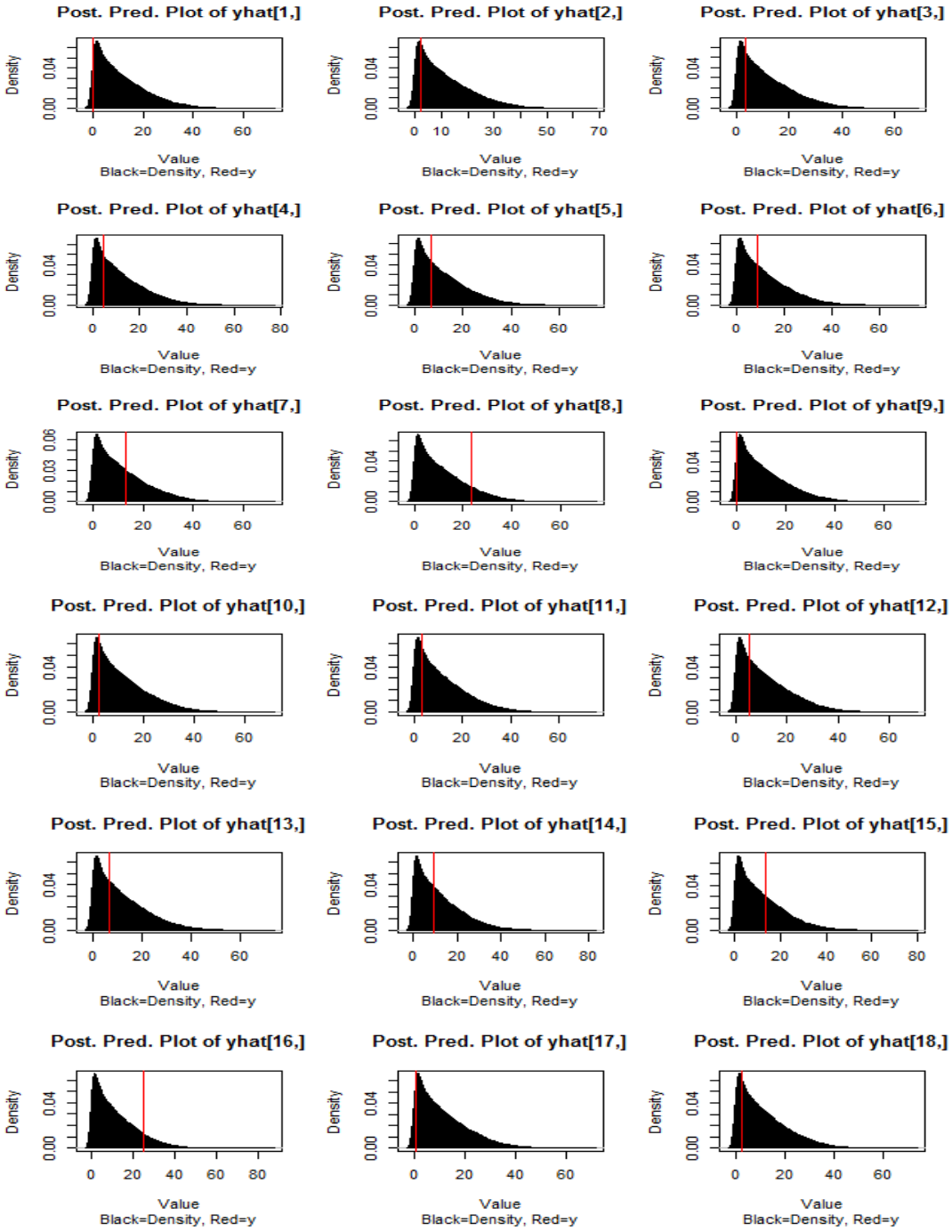

Figure 11. Posterior predictive distributions (black) and observed values (red lines) for remission times $\hat{y}_i$, showing model adequacy across observations 1 to 18 (Bladder cancer data, $N = 137$).

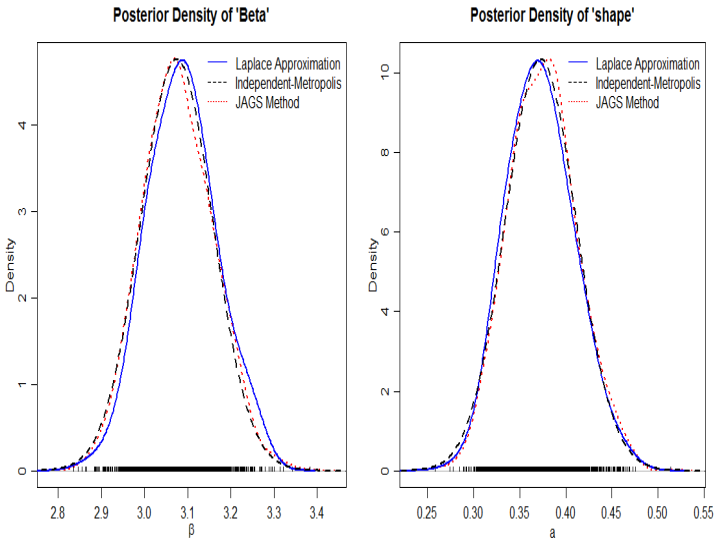

Figure 12. Posterior density for β parameter (left) and shape parameter a (right) estimated via Laplace Approximation (solid line, blue), Independent Metropolis (dashed line, green), and JAGS (dotted line, red) methods (IUD discontinuation dataset, $N = 18$).

estimation approaches confirms the robustness of the exponentiated Rayleigh model and the reliability of the Bayesian inference procedures used.

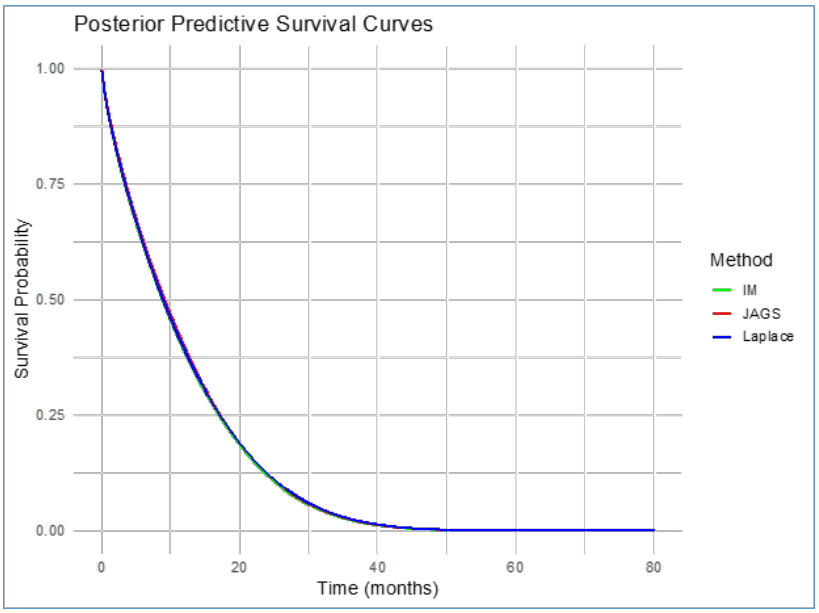

Figure 13. Posterior predictive survival curves for bladder cancer data fitted using the exponentiated Rayleigh model. Results are shown for Laplace Approximation (blue), Independence Metropolis (green), and JAGS (red) methods. Shaded regions represent 95% credible intervals for each approach.

The results suggest that the highest risk period for bladder cancer patients occurs shortly after intervention, aligning well with clinical expectations. This pattern reinforces the importance of early monitoring and intervention post-treatment.

10. Discussion

The findings of this study demonstrate the effectiveness of the exponentiated Rayleigh distribution for modeling survival data with right-censored medical observations. Through comprehensive comparisons between Bayesian and maximum likelihood estimation approaches, we established that both frameworks produce consistent parameter estimates, validating the reliability of the exponentiated Rayleigh model. However, Bayesian inference, particularly the Independent Metropolis algorithm gave more stable and informative estimates, offering tighter uncertainty bounds and stronger diagnostic performance than classical methods. . This improved uncertainty quantification is especially valuable in clinical concept where risk assessment must be both valid and interpretable.

A key methodological contribution of this research is the consistent robustness of the Independent Metropolis algorithm, which outperformed other Bayesian techniques in terms of both computational efficiency and statistical precision. The algorithm's performance suggests that carefully implemented Markov chain Monte Carlo methods with optimized proposal distributions should be preferred when exact posterior inference is required for survival analysis. Diagnostic measures including Bayesian p-values near 0.5 for both datasets and excellent convergence metrics ($\hat{R} < 1.01$) further confirmed the model's appropriateness, supporting its adoption for real-world clinical research applications. These diagnostics collectively verify that the model captures essential properties of the underlying survival mechanisms without exhibiting systematic misfit.

The shape parameter estimates revealed clinically meaningful patterns in both applications. For the intrauterine device discontinuation data, the estimated shape parameter between 0.7 and 0.8 indicated a moderately increasing hazard function, consistent with progressive risk accumulation as time-on-device increases. In contrast, the bladder cancer remission data showed a decreasing hazard pattern with a shape parameter around 0.37, consistent with clinical expectations where the highest risk of recurrence typically occurs shortly after treatment. These distinct hazard patterns demonstrate the exponentiated Rayleigh model's flexibility in adapting to different survival scenarios, reinforcing its suitability for modeling medical time-to-event outcomes with non-constant hazards.

This research established the exponentiated Rayleigh survival model as a robust tool for analyzing censored medical data, capable of capturing various hazard rate patterns. The Bayesian framework, especially when implemented through the Independent Metropolis algorithm, proved particularly valuable by delivering precise and interpretable posterior estimates while maintaining reasonable computational demands. The shape parameter emerged as a key indicator of underlying risk patterns, with its interpretation providing clinically relevant insights that could inform patient monitoring strategies and treatment decisions. These findings underscore the value of pairing flexible parametric models with modern Bayesian computation in clinical research.

Several important implications emerge from these findings. First, the exponentiated Rayleigh model shows particular promise for medical survival analysis applications where data exhibit non-constant hazard rates. Second, Bayesian methods generally offer advantages over maximum likelihood estimation, especially through their ability to provide full posterior distributions rather than point estimates with asymptotic approximations. Third, the shape parameter's clinical interpretability enhances the model's utility for medical decision-making by directly relating to patient risk patterns over time. Together, these strengths position the model as a practical and statistically rigorous option for applied medical researchers.

Future research directions should explore several extensions of this work. Incorporating additional covariates into the model framework would enable more personalized risk predictions by accounting for patient-specific factors. Investigating alternative prior distributions might further improve the model's robustness across different clinical scenarios. Comparative studies applying the Independent Metropolis algorithm to other survival distributions could help establish its general effectiveness for Bayesian survival analysis. Additionally, applications to larger datasets and different medical conditions would further test the model's generalizability and stability.

For applied researchers and clinical investigators, we recommend adopting the exponentiated Rayleigh model with Bayesian estimation, particularly using the Independent Metropolis algorithm, when analyzing time-to-event medical data. This approach combines statistical rigor with practical interpretability, providing results that can directly inform clinical understanding and decision-making. Reporting should include full posterior summaries alongside traditional point estimates to provide comprehensive characterization of uncertainty. Model validation through diagnostic checks remains essential to ensure reliable conclusions.

11. Conclusion

In conclusion, this research presents a statistically sound and clinically relevant framework for survival analysis in medical research. The exponentiated Rayleigh model, particularly when implemented through Bayesian methods, offers researchers and clinicians a powerful tool for understanding time-to-event outcomes. The model's flexibility in capturing different hazard patterns, combined with the methodological advantages of modern computational statistics, positions it as a valuable addition to the analytical toolkit for medical research. Future extensions and broader applications hold strong potential to advance practical inference in medical survival analysis and to deepen clinical insight into disease progression and treatment response.

Acknowledgement

The authors would like to express their sincere gratitude to the editors and anonymous reviewers for their constructive comments and valuable suggestions, which substantially improved the quality and clarity of this manuscript. We also acknowledge the developers of the `R` and `Stan` statistical software and associated packages used in this study for providing open-source tools that made the computational analyses possible. Finally, we thank the original data contributors for making the datasets publicly available, thereby enabling reproducible and transparent research.

Appendix

Functions for Exponetiated Rayleigh (expRay) Model in R

1. R code for cumulative distribution function (cdf)

```
pexpRay <- function(x, a, lambda){
            p <- (1-exp(-(x/lambda)^2))^a
            return(p)
         }
```

2. R code for probability density function (pdf)

```
dexpRay <- function(x, a, lambda){
            d <-   2*a*(x/lambda^2)*exp(-(x/lambda)^2)*
            (1-exp(-(x/lambda)^2))^a-1
            return(d)
        }
```

3. R code for random generation function (rng)

```
rexpRay <- function(n, a, lambda){
```

```
    u <- runif(n)
    x <- lambda*(-log(1-u^(1/a)))^(1/2)
    return(x)
}
```

4. R code for survival function

```
SurvexpRay <- function(x, a, lambda){
    s <- 1-(1-exp(-(x/lambda)^2))^a
    return(s)
}
```

5. R code for hazard function

```
hexpRay <- function(x, a, lambda){
    h<-dexpRay(x,a,lambda)/SurvexpRay(x,a,lambda)
    return(h)
}
```

REFERENCES

1. M. T. Akhtar and A. A. Khan, *Bayesian analysis of generalized log-Burr family with R*, SpringerPlus, vol. 3, p. 185, 2014.
2. M. T. Akhtar and A. A. Khan, *Log-logistic distribution as a reliability model: A Bayesian analysis*, American Journal of Mathematics and Statistics, vol. 4, no. 3, pp. 162–170, 2014.
3. M. T. Akhtar and A. A. Khan, *Bayesian analysis of Poisson reliability model with R and JAGS*, International Journal of Recent Scientific Research, vol. 8, no. 11, pp. 21837–21841, 2017.
4. M. T. Akhtar and A. A. Khan, *Bayesian reliability analysis of binomial model: Application to success/failure data*, Journal of Modern Applied Statistical Methods, vol. 17, no. 2, eP2623, 2018.
5. N. E. Abd El Hady, *Exponentiated transmuted Weibull distribution*, International Journal of Mathematical, Computational, Statistical, Natural and Physical Engineering, vol. 8, no. 6, 2014.
6. I. B. Abdul-Moniem, *Recurrence relations for moments of lower generalized order statistics from exponentiated Lomax distribution and its characterization*, Journal of Mathematical and Computational Science, vol. 2, pp. 999–1011, 2012.
7. A. Alzaghal, F. Famoye, and C. Lee, *Exponentiated T-X family of distributions with some applications*, International Journal of Statistics and Probability, vol. 2, no. 3, pp. 31–49, 2013.
8. N. Bleistein and R. Handelsman, *Asymptotic Expansions of Integrals*, Dover Publications, New York, 1986.
9. D. Collett, *Modelling Survival Data in Medical Research*, Chapman & Hall, London, 3rd edition, 2015.
10. I. Elbatal and H. Z. Muhammed, *Exponentiated generalized inverse Weibull distribution*, Applied Mathematical Sciences, vol. 8, no. 81, pp. 3997–4012, 2014.
11. R. C. Gupta, P. L. Gupta, and R. D. Gupta, *Modeling failure time data by Lehman alternatives*, Communications in Statistics – Theory and Methods, vol. 27, no. 4, pp. 887–904, 1998.
12. R. D. Gupta and D. Kundu, *Generalized exponential distributions*, Australian and New Zealand Journal of Statistics, vol. 41, no. 2, pp. 173–188, 1999.
13. W. K. Hastings, *Monte Carlo sampling methods using Markov chains and their applications*, Biometrika, vol. 57, no. 1, pp. 97–109, 1970.
14. N. Khan, M. T. Akhtar, and A. A. Khan, *A Bayesian approach to survival analysis of inverse Gaussian model with Laplace approximation*, International Journal of Statistics and Applications, vol. 6, no. 6, pp. 391–398, 2016.
15. N. Khan, M. T. Akhtar, and A. A. Khan, *Bayesian analysis of Marshall–Olkin family of distributions*, International Journal of Recent Scientific Research, vol. 8, no. 7, pp. 18692–18699, 2017.
16. N. Khan and A. A. Khan, *Bayesian analysis of Topp–Leone generalized exponential distribution*, Austrian Journal of Statistics, vol. 47, no. 4, pp. 1–15, 2018.
17. N. Khan and A. A. Khan, *A Bayesian approach to survival analysis of Gompertz model with R and JAGS*, Information Sciences Letters, vol. 12, no. 3, pp. 1479–1496, 2023.
18. H. S. Klakattawi, *Survival analysis of cancer patients using a new extended Weibull distribution*, PLoS ONE, vol. 17, no. 2, e0264229, 2022.
19. E. T. Lee and J. W. Wang, *Statistical Methods for Survival Data Analysis*, Wiley-Interscience, 3rd edition, 2003.

20. A. J. Lemonte, W. Barreto-Souza, G. M. Cordeiro, et al., *The exponentiated Kumaraswamy distribution and its log-transform*, Brazilian Journal of Probability and Statistics, vol. 27, no. 1, pp. 31–53, 2013.
21. J. Liang, *Hastings-within-Gibbs algorithm: Introduction and application on hierarchical model*, University of Texas at San Antonio, 2010.
22. D. Lunn, C. Jackson, N. Best, A. Thomas, and D. Spiegelhalter, *The BUGS Book: A Practical Introduction to Bayesian Analysis*, Chapman & Hall/CRC, Boca Raton, FL, 2013.
23. M. Mahmoud and M. Ghazal, *Estimations from the exponentiated Rayleigh distribution based on generalized type-II hybrid censored data*, Journal of the Egyptian Mathematical Society, vol. 25, no. 1, pp. 71–78, 2017.
24. G. S. Mudholkar, D. K. Srivastava, and M. Freimer, *The exponentiated Weibull family: A reanalysis of the bus-motor-failure data*, Technometrics, vol. 37, no. 4, pp. 436–445, 1995.
25. S. Nadarajah, *The exponentiated Gumbel distribution with climate application*, Environmetrics, vol. 17, no. 1, pp. 13–23, 2006.
26. S. Nadarajah, *The exponentiated exponential distribution: A survey*, AStA Advances in Statistical Analysis, vol. 95, pp. 219–251, 2011.
27. S. Nadarajah and A. K. Gupta, *The exponentiated gamma distribution with application to drought data*, Calcutta Statistical Association Bulletin, vol. 59, no. 1–2, pp. 29–54, 2007.
28. S. Nadarajah and S. Kotz, *The exponentiated Fréchet distribution*, InterStat Electronic Journal, vol. 14, pp. 1–7, 2003.
29. S. Nadarajah and S. Kotz, *The beta exponential distribution*, Reliability Engineering and System Safety, vol. 91, no. 6, pp. 689–697, 2006.
30. M. Nassar and A. Elshahhat, *Statistical analysis of inverse Weibull constant-stress partially accelerated life tests with adaptive progressively type-I censored data*, Mathematics, vol. 11, no. 2, pp. 1–29, 2023.
31. J. C. Nash, *On best practice optimization methods in R*, Journal of Statistical Software, vol. 60, no. 2, pp. 1–14, 2014.
32. I. Ntzoufras, *Bayesian Modeling Using WinBUGS*, John Wiley & Sons, New York, 2009.
33. M. Plummer, *JAGS: A program for analysis of Bayesian graphical models using Gibbs sampling*, Proceedings of the 3rd International Workshop on Distributed Statistical Computing, Vienna, 2003.
34. M. Plummer, *JAGS version 3.3.0 user manual*, International Agency for Research on Cancer, Lyon, France, 2012.
35. M. Plummer, *rjags: Bayesian graphical models using MCMC*, R package version 4-10, 2023.
36. R Core Team, *R: A language and environment for statistical computing* (Version 4.4.2), R Foundation for Statistical Computing, Vienna, Austria, 2024.
37. M. M. Ristić and N. Balakrishnan, *The gamma-exponentiated exponential distribution*, Journal of Statistical Computation and Simulation, vol. 82, no. 8, pp. 1191–1206, 2011.
38. E. Ruli, N. Sartori, and L. Ventura, *Improved Laplace approximation for marginal likelihoods*, Electronic Journal of Statistics, vol. 10, no. 2, pp. 3986–4009, 2016.
39. A. Shawky and H. H. Abu-Zinadah, *Exponentiated Pareto distribution: Different methods of estimations*, International Journal of Contemporary Mathematical Sciences, vol. 4, no. 14, pp. 677–693, 2009.
40. Statisticat, LLC, *Bayesian inference*, R package version 16.1.6, 2021.
41. Y. Su and M. Yajima, *R2jags: Using R to run JAGS*, R package version 0.7-1, 2021.
42. M. G. M. Ghazal and M. M. Hasaballah, *Bayesian estimations using MCMC approach under exponentiated Rayleigh distribution based on unified hybrid censored scheme*, Journal of Statistical Applications and Probability, vol. 6, no. 2, pp. 329–344, 2017.
43. P. Kumari, V. Kumar, R. Kundu, and P. Kumar, *Bayesian estimation of exponentiated Rayleigh distribution under symmetric and asymmetric loss functions*, Current Journal of Applied Science and Technology, vol. 41, no. 48, pp. 82–90, 2022.
44. J. A. Darwish, *Statistical properties and applications for exponentiated exponential Rayleigh distribution*, Thermal Science, vol. 28, no. 6B, pp. 4895–4906, 2024.
45. R. K. Joshi and G. P. Dhungana, *Exponentiated Rayleigh Poisson distribution: Model, properties and applications*, American Journal of Theoretical and Applied Statistics, vol. 9, no. 6, pp. 272–282, 2020.
46. Stan Development Team, *RStan: the R interface to Stan*, R package version 2.32.6, 2024. https://mc-stan.org/.
47. D. Machin, C. D'arcangues, B. Busca, T. M. M. Farley, and A. Pinol, *Vaginal bleeding patterns —— the problem and an example data set*, Applied Stochastic Models and Data Analysis, vol. 3, no. 1, pp. 27–35, 1987. https://doi.org/10.1002/asm.3150030104.
48. F. Bartoš, F. Aust, and J. M. Haaf, *Informed Bayesian survival analysis*, BMC Medical Research Methodology, vol. 22, article 238, 2022. https://doi.org/10.1186/s12874-022-01676-9
49. I. Paolucci, Y. M. Lin, J. A. M. Silva, et al., *Bayesian parametric models for survival prediction in medical applications*, BMC Medical Research Methodology, vol. 23, article 250, 2023. https://doi.org/10.1186/s12874-023-02059-4
50. S. Farhin, M. Ashraf-Ul-Alam, and A. A. Khan, *Bayesian Modelling of Exponentiated Weibull Generated Family for Interval-Censored Data with rstan*, Thailand Statistician, vol. 21. no. 4, pp. 783–801, 2024. https://ph02.tci-thaijo.org/index.php/thaistat/article/view/251054